Interpretation of states in ^{105}Ag utilizing a particle-rotor model

Sadek Zeghib, F. A. Rickey, and P. C. Simms
Tandem Accelerator Laboratory, Purdue University, Lafayette, Indiana 47907
(Received 2 April 1986)

Previously observed positive and negative parity states of ^{105}Ag have been interpreted using a particle-rotor model. Experimental energies and transition properties have been compared to those predicted by the calculation. The results show that this simple model with very few parameters can explain successfully most of the structure of ^{105}Ag. Most members of the multiplets resulting from the coupling of $R=0$, 2, and 4 excitations of the core to $g_{9/2}$, $f_{5/2}$, $p_{3/2}$, and $p_{1/2}$ orbitals have been identified.

I. INTRODUCTION

In previous work[1] utilizing (HI,$xn\gamma$) reactions high spin states on or near the yrast line have been identified in ^{105}Ag. Energy levels, branching ratios, multipole mixing ratios and lifetimes were calculated using a slightly deformed rotor model. The agreement with the experimental data was very good.

More insight into the nature of nuclear structure can be gained from non-yrast states. The rotational model, for example, predicts specific systematics for non-yrast states in odd-A nuclei depending on whether the shell is nearly empty or nearly full. Odd-neutron nuclei in this mass region typically contain only a few particles outside of the closed $N=50$ shell, while for odd-proton nuclei the $Z=50$ shell is almost full. Thus while they share the same core, ^{105}Ag is expected to exhibit different systematics than ^{105}Pd. An extensive set of low spin states in ^{105}Ag have been identified from the β^+ decay of ^{105}Cd,[2] (α,2nγ) reactions,[3,4] and the (p,t) reaction.[5] The present work describes an extension of the rotational calculations to this set of non-yrast states.

II. MODEL CALCULATION

A simple rotational model obviously cannot describe all of the states present, since it does not include non-rotational states of the core. Nevertheless it is attractive since properties of γ-ray transitions can readily be calculated. The specific model used here employs a standard rotational Hamiltonian in the strong coupling limit modified to include a variable moment of inertia. The single-particle basis states are obtained from a standard Nilsson calculation,[6] and pairing is treated in the BCS approximation. Coriolis and recoil terms are treated to all orders, and mix the basis states to produce the final calculated states. Energies and wave functions are calculated according to Smith and Rickey,[7] and transition properties according to Popli *et al.*[1]

At small deformations Coriolis mixing is substantial, so that the traditional Nilsson asymptotic quantum numbers are no longer an appropriate label for the final states. Although neither the core angular momentum R nor the particle angular momentum j is a good quantum number in the strong coupling limit, the calculated wave functions contain a dominant R and j value due to the Coriolis interaction. This allows us to describe the complete set of states calculated as the coupling of each single particle state to the ground and excited states of the core. Thus in the remainder of this paper we will use the language of shell-model particle-core multiplets even though the actual calculation is a rotational one.

The parameters used in the calculation were constrained by the requirement that both yrast and non-yrast states be satisfactorily described. Thus the parameters of the previous calculation[1] at a deformation of $\delta=0.12$ were retained in the present calculation. The Fermi surface λ and the elastic constant C of the variable moment of inertia (VMI) model have been changed slightly. The Fermi surface is presently taken to be 40.55 or 40.35 MeV for the positive or negative states, respectively, instead of 40.5 MeV for both parities, and C has been changed to 6.5×10^{-7} keV^3 from 5.2×10^{-7} keV^3 for the positive parity states.

The Nilsson diagram for protons in ^{105}Ag is shown in Fig. 1, where the approximate location of the Fermi surface is shown as a heavy horizontal line. At a deformation of $\delta=0.12$ positive parity states from other $N=4$ orbitals ($d_{5/2}$, $g_{7/2}$, etc.) are expected at much higher energies. Thus the only positive-parity states included in the basis were the five states of $g_{9/2}$ parentage. For negative-parity states the basis included all states with $p_{1/2}$, $p_{3/2}$, and $f_{5/2}$ parentage. Preliminary calculations showed that states of $f_{7/2}$ parentage had negligible amplitudes in the final wave functions, and they were not included in the basis for the calculations presented here.

The model calculation gives, in addition to the final energy, the composition of each final state in terms of the basis states, and also the contribution of various core rotations ($R=0,2,4,\ldots$) to each final state. This permits the straightforward identification of calculated states as members of the various multiplets. Transition properties are also calculated, which assists the comparison of theory and experiment.

III. DISCUSSION OF THE RESULTS

The experimental quantities available for the comparison to model predictions were spins and parities, level en-

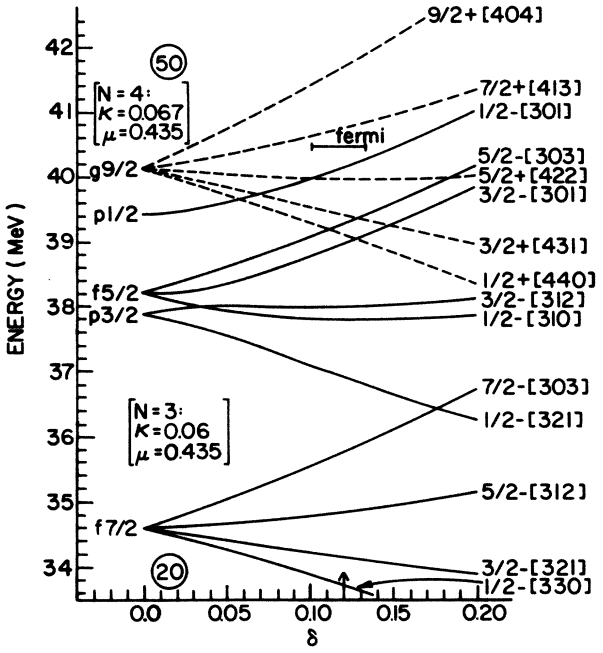

FIG. 1. Nilsson diagram for protons in ^{105}Ag. The heavy horizontal bar shows the approximate position of the Fermi surface.

ergies, and relative γ-ray intensities. Level energies are a less reliable basis for comparison than the branching ratios describing the decay of the state. Small effects not included in the calculation can affect energies substantially without seriously changing the wave function, as is known from perturbation theory. Branching ratios are more sensitive to the wave functions, and provide a more characteristic signature of the states. (Transition probabilities, of course, are also sensitive to the transition energies. Thus in our calculations we use theoretical wave functions, but experimental transition energies whenever possible.)

A few examples are listed in Table I to illustrate the importance of branching ratios. The first example concerns $9/2^-$ states. The calculated energies of the lowest two $9/2^-$ states differ by only 159 keV (1149 and 1298 keV), and bracket the energy of the lowest observed $9/2^-$ state (1166 keV). Thus on the basis of energy alone a clear-cut association between experiment and theory cannot be made. The branching ratio comparison clearly favors the lower $9/2^-$ state of the calculation. In the second example the theory predicts the three lowest $7/2^+$ states at the following energies: the $7/2_1^+$ at 305 keV, the $7/2_2^+$ at 1262 keV, and the $7/2_3^+$ at 2497 keV. The branching ratios of Table I show that the experimental $7/2^+$ state at 1922 keV is best described by the calculated $7/2_2^+$ state, although the calculated energy is too low. The observed $7/2^+$ state at 2419 keV is best identified as the calculated $7/2_3^+$ state. The differences in calculated branching ratios for the three $7/2^+$ states and the three $9/2^-$ states are due to the composition of their wave functions in terms of the basis states. Table II clearly shows that the wave functions are completely different which results in different decay properties. Thus in our comparisons we insist that the energy match must be sensible, but use branching ratios (where available) as the primary criterion.

Unfortunately, many of the negative-parity states expected were not populated in either β-decay or $(\alpha,2n\gamma)$ reactions. We would like to see if the model predictions for multiplets involving $p_{1/2}$, $p_{3/2}$, and $f_{5/2}$ orbitals are sensible. A large set of negative-parity states were observed in the (p,t) reaction.[5] Assignments of these states to specific multiplets cannot be as reliable since there is less basis for comparison of experiment and theory. Branching ratios obviously were not observed, and the actual spins were not measured. There is, however, additional information available from the measured cross-sections. The ground

TABLE I. Comparison of experimental and calculated branching ratios for selected states.

I_i^π	I_f^π	E_γ (keV)	Experimental	Branching ratios for Calculated (favored)	Calculated	Calculated
			$9/2^-(1166)$	$9/2_1^-(1149)$	$9/2_2^-(1298)$	$9/2_3^-(1785)$
$9/2^-$	$5/2^-$	733	1.00	0.99	0.69	0.00
	$7/2^-$	143	0.00	0.01	0.31	1.00
			$7/2^+(1922)$	$7/2_2^+(1262)$	$7/2_3^+(2497)$	
$7/2^+$	$7/2^+$	1897	0.61	0.65	0.65	
	$9/2^+$	1870	0.29	0.28	0.06	
	$9/2_2^+$	826	0.05	0.04	0.28	
	$5/2_2^+$	252	0.06	0.03	0.01	
			$7/2^+(2419)$	$7/2_3^+(2497)$	$7/2_2^+(1262)$	
$7/2^+$	$7/2^+$	2394	0.46	0.39	0.56	
	$5/2^+$	1432	0.11	0.09	0.12	
	$9/2_2^+$	1322	0.15	0.31	0.05	
	$3/2^+$	1033	0.18	0.10	0.04	
	$5/2_2^+$	748	0.10	0.11	0.26	

TABLE II. Composition of the wave functions for the calculated $7/2^+$ and $9/2^-$ states.

I_i^π	E_i (keV)	Nilsson basis states					
		$1/2^+[440]$	$3/2^+[431]$	$5/2^+[422]$	$7/2^+[413]$	$9/2^+[403]$	
$7/2_1^+$	305	0.01	0.09	0.33	0.57		
$7/2_2^+$	1262	0.08	0.39	0.17	0.36		
$7/2_3^+$	2497	0.26	0.22	0.45	0.07		
		$1/2^-[301]$	$1/2^-[310]$	$1/2^-[321]$	$3/2^-[301]$	$3/2^-[312]$	$5/2^-[303]$
$9/2_1^-$	1149	0.80	0.03	0.00	0.03	0.04	0.10
$9/2_2^-$	1298	0.17	0.00	0.00	0.10	0.03	0.69
$9/2_3^-$	1785	0.00	0.10	0.00	0.75	0.00	0.14

state of ^{107}Ag has spin and parity $1/2^-$. Thus the largest cross-sections to states in ^{105}Ag should involve couplings of a $p_{1/2}$ proton to excited states of the ^{104}Pd core. In a rotational interpretation the ground state of ^{107}Ag is not simply a $p_{1/2}$ proton, but an $\Omega=1/2$ Nilsson state (the $1/2^-[301]$). At the deformation utilized in the present calculation this state contains a 7% contribution of $p_{3/2}$ and an 8% contribution of $f_{5/2}$ orbitals. Thus smaller cross-sections to states in ^{105}Ag involving $p_{3/2}$ and $f_{5/2}$ orbitals are reasonable. We have used this cross-section information in a very qualitative way. If a state observed with the appropriate energy and "spin" has a small cross-section (for the corresponding ℓ-transfer) we regard it as a candidate for a $p_{3/2}$ or $f_{5/2}$ coupling. The large cross-sections must correspond to $p_{1/2}$ couplings. As will be seen below, our calculated $p_{1/2}$ multiplets fit this criterion beautifully. Because of this, we have elected to include the (p,t) data in our analysis, associating less confidence in the conclusions.

The final results are given in Fig. 2 and Tables III–V. Figure 2 shows the states identified as members of the $R=0$, 2, 4, and 6 multiplets based on the $g_{9/2}$ orbital. The dashed curves connect the calculated energies.

Tables III–V compare experimental observables to the calculated ones. The final columns of each of Tables III–V give the multiplet identification of each observed state. Table III presents experimental energies, spins, and branching ratios from β decay and $(\alpha,2n\gamma)$ reactions, along with the appropriate calculated quantities. The overall agreement between the calculated and experimental results is very good, particularly for the branching ratios. Table IV includes experimental energies, spins, and cross-sections from the (p,t) reaction. There is some repetition, notably for $p_{1/2}$ states, in order to present the cross-section data. We have made no attempt to calculate cross-sections, since this is a difficult task. We can, however, estimate the magnitude of the expected cross-sections from the overlap of the initial and final wave functions. As was discussed earlier, the largest cross-sections are expected for $p_{1/2}$ dominated states, and this is the case. The observed cross-sections to states we associate with $p_{3/2}$ and $f_{5/2}$ multiplets are typically smaller by roughly an order of magnitude, which would be suggested by the calculated wave functions. There is one exception, the $9/2^-$ state at 1757 keV. It is interesting to note that the calculated wave function for this state contains a larger $p_{1/2}$ component than normal.

A measure of the overall success of the model interpretation is that all but one of the low-lying states predicted have been identified among those observed. We have identified complete multiplets for the coupling of $g_{9/2}$, $p_{1/2}$, and $p_{3/2}$ protons to the $R=0$, 2 and 4 states of the core and for the coupling of an $f_{5/2}$ proton to the $R=0$ and 4 states of the core. The only member of the $f_{5/2}$,$R=2$ multiplet we cannot identify is the $7/2^-$ member predicted to lie at 915 keV. Several members of the $g_{9/2}$, $R=6$ multiplet have been identified. The missing members should lie at higher excitation energies where they would be difficult to populate.

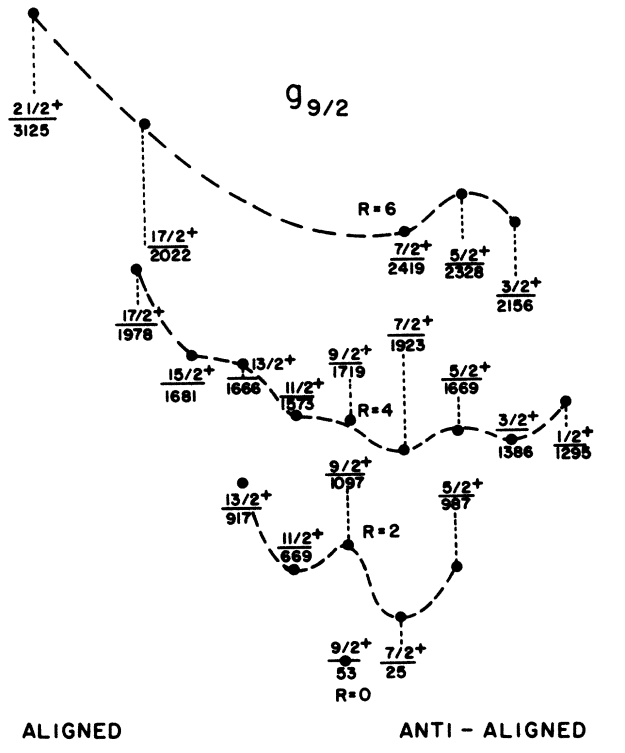

FIG. 2. States identified as members of the $R=0$, 2, 4 and 6 multiplets based on $g_{9/2}$ particles. Solid horizontal lines represent experimental energies. The dashed curves connect the calculated energies shown as dots.

TABLE III. Comparison between experimental and calculated results. The experimental values are taken from Ref. 2 unless otherwise noted.

E_i (keV)		I_i^π	I_f^π	E_γ (keV)	Branching ratio		ℓ_j	R projection
Expt.	Theor.				Expt.	Theor.		
0.0	0.0[f]	$1/2^-$					$p_{1/2}$	$R=0$
25.5	305	$7/2^+$					$g_{9/2}$	$R=2$
53.2	53.2[f]	$9/2^+$	$7/2^+$	028	1.00	1.00	$g_{9/2}$	$R=0$
346.9	356	$3/2^-$	$1/2^-$	347	1.00	1.00	$p_{1/2}$	$R=2$
433.2	443	$5/2^-$	$1/2^-$	433.2	0.95	0.999	$p_{1/2}$	$R=2$
			$3/2^-$	86	0.05	0.001		
668.6[a]	573	$11/2^+$	$9/2^+$	616	1.00[a]	0.98	$g_{9/2}$	$R=2$
			$7/2^+$	644	0.00	0.02		
877.8	817	$3/2_2^-$	$1/2^-$	877.8	0.70	0.83	$p_{3/2}$	$R=0$
			$3/2^-$	531	0.24	0.14		
			$5/2^-$	444	0.06	0.03		
917.3[a]	1063	$13/2^+$	$11/2^+$	249	0.24[a]	0.45	$g_{9/2}$	$R=2$
			$9/2^+$	864	0.76	0.55		
987.3	600	$5/2^+$	$7/2^+$	962	0.79	0.99	$g_{9/2}$	$R=2$
			$9/2^+$	934	0.21	0.01		
1023.7	1045	$7/2_2^-$	$5/2^-$	590	0.71	0.58	$p_{1/2}$	$R=4$
			$3/2^-$	677	0.29	0.42		
1042.7[b]	606	$5/2_2^-$	$5/2^-$	609	0.79[b]	0.41	$f_{5/2}$	$R=0$
			$3/2^-$	696	0.21	0.59		
1097.1	700	$9/2_2^+$	$9/2^+$	1044	0.18	0.04	$g_{1/2}$	$R=2$
			$7/2^+$	1072	0.82	0.96		
1166.3	1149	$9/2^-$	$7/2^-$	143	0.00	0.01	$p_{1/2}$	$R=4$
			$5/2^-$	733	1.00	0.99		
1243.4	1090	$5/2_3^-$	$5/2^-$	810	0.59	0.33	$p_{3/2}$	$R=2$
			$3/2^-$	897	0.41	0.67		
1294.9	1568	$1/2^+$	$5/2^+$	308	1.00	1.00	$g_{9/2}$	$R=4$
1386.3	1343	$3/2^+$	$5/2^+$	399	0.10	0.38	$g_{9/2}$	$R=4$
			$7/2^+$	1361	0.90	0.62		
1416	1564	$3/2_3^-$	$1/2^-$	1416	1.00	0.61	$f_{5/2}$	$R=2$
			$3/2^-$	1069	0.00	0.25		
			$3/2_2^-$	538	0.00	0.04		
			$5/2^-$	983	0.00	0.09		
			$5/2_2^-$	373	0.00	0.01		
1572.7[c]	1457	$11/2_2^+$	$9/2^+$	1520	0.37[c]	0.46	$g_{9/2}$	$R=4$
			$7/2^+$	1546	0.63	0.54		
1666.1[c]	1737	$13/2_2^+$	$13/2^+$	748	0.21[c]	0.43	$g_{9/2}$	$R=4$
			$11/2^+$	997	0.57	0.38		
			$9/2^+$	1612	0.22	0.19		
1669.5	1385	$5/2_2^+$	$7/2^+$	1644	0.82	0.65	$g_{9/2}$	$R=4$
			$5/2^+$	682	0.03	0.15		
			$3/2^+$	283	0.15	0.20		
1681.2[a]	1783	$15/2^+$	$13/2^+$	764	0.70[a]	0.77	$g_{9/2}$	$R=4$
			$11/2^+$	1012	0.30	0.23		
1718.8	1433	$9/2_3^+$	$9/2^+$	1666	0.10	0.27	$g_{9/2}$	$R=4$
			$7/2^+$	1693	0.90	0.73		
1922.9	1262	$7/2_2^+$	$7/2^+$	1897	0.61	0.65	$g_{9/2}$	$R=4$
			$9/2^+$	1870	0.28	0.28		
			$9/2_2^+$	826	0.05	0.04		
			$5/2_2^+$	253	0.06	0.03		
1978.1[a]	2284	$17/2^+$	$15/2^+$	297	0.12[a]	0.24	$g_{9/2}$	$R=4$
			$13/2^+$	1061	0.88	0.76		
2022.6[a]	3113	$17/2_2^+$	$15/2^+$	341	0.25[a]	0.14	$g_{9/2}$	$R=6$
			$13/2^+$	1105	0.75	0.86		
2113.4[b,d]	1785	$9/2_3^-$	$11/2^-$	107[e]	0.00	0.002	$p_{3/2}$	$R=4$
			$9/2^-$	947	1.00[b]	0.998		
2144.4	2175	$5/2_5^-$	$3/2^-$	1797	1.00	0.92	$f_{5/2}$	$R=4$
			$3/2_2^-$	1266	0.00	0.03		

TABLE III. (*Continued.*)

E_i (keV) Expt.	E_i (keV) Theor.	I_i^π	I_f^π	E_γ (keV)	Branching ratio Expt.	Branching ratio Theor.	ℓ_j	R projection
			$7/2^-$	1121	0.00	0.03		
			$5/2_3^-$	901	0.00	0.02		
2156.4	2583	$3/2_2^+$	$5/2^+$	1169	0.48	0.30	$g_{9/2}$	$R=6$
			$3/2^+$	770	0.24	0.36		
			$5/2_2^+$	487	0.28	0.34		
2327.8	2736	$5/2_3^+$	$5/2^+$	1340	0.77	0.41	$g_{9/2}$	$R=6$
			$3/2^+$	942	0.15	0.40		
			$5/2_2^+$	658	0.08	0.19		
2419.1	2497	$7/2_3^+$	$7/2^+$	2394	0.46	0.39	$g_{9/2}$	$R=6$
			$5/2^+$	1432	0.11	0.09		
			$9/2_2^+$	1322	0.15	0.31		
			$3/2^+$	1033	0.18	0.10		
			$5/2_2^+$	749	0.10	0.11		
3125.1[a]	3723	$21/2^+$	$19/2^+$	281[e]	0.00	0.15	$g_{9/2}$	$R=6$
			$17/2^+$	1147	1.00[a]	0.85		

[a]Reference 1.
[b]Reference 3.
[c]Reference 4.
[d]Reference 5.
[e]Transition energy is not known experimentally; calculated value has been used.
[f]The calculated energies of $9/2^+$ and $1/2^-$ states have been adjusted to the experimental ones.

Also listed (in Table V) are states observed in the β^+ decay of ^{105}Cd (up to 2250 keV) which could not be identified. These states all have different branching ratios than any calculated state of the appropiate spin, and thus seem to be of a different character than those identified. We believe that these states are non-rotational and might come from the (2',4',...) core excited states which our rotational model cannot account for.

IV. ROTATIONAL SYSTEMATICS

In a rotational calculation at small deformations the relative energies of states in a particular multiplet are dictated primarily by the position of the Fermi surface in the Nilsson basis and the form of the Coriolis interaction. The systematics of these effects are most conveniently discussed for the case of unique-parity orbitals ($g_{9/2}$ paren-

TABLE IV. Identification of observed negative parity states from the (p,t) reaction (Ref. 5).

E_i Expt.[a]	E_i Theor.	I_i^π Expt.	I_i^π Theor.	σ ($\mu b/sr$)	ℓ_j	R projection
346	356	$3/2^-$	$3/2^-$	30	$p_{1/2}$	$R=2$
433	443	$5/2^-$	$5/2^-$	43	$p_{1/2}$	$R=2$
1023	1045	$7/2^-$	$7/2_2^-$	6.9	$p_{1/2}$	$R=4$
1166	1149	$9/2^-$	$9/2^-$	10	$p_{1/2}$	$R=4$
1327	1678	$(11/2,13/2)^-$	$11/2^-$	0.7	$f_{5/2}$	$R=4$
1643	1424	$(7/2,9/2)^-$	$7/2_3^-$	1.8	$p_{3/2}$	$R=2$
1706	1705	$(3/2,5/2)^-$	$5/2_4^-$	4.0	$f_{5/2}$	$R=2$
1757	1298	$(7/2,9/2)^-$	$9/2_2^-$	19	$f_{5/2}$	$R=2$
1921	2001	$(11/2,13/2)^-$	$13/2^-$	1.2	$f_{5/2}$	$R=4$
1959	1709	$1/2^-$	$1/2_2^-$	9.0	$f_{5/2}$	$R=2$
2029	2288	$(7/2,9/2)^-$	$9/2_4^-$	6.0	$f_{5/2}$	$R=4$
2086	1916	$(3/2,5/2)^-$	$3/2_4^-$	9.5	$p_{3/2}$	$R=2$
2113	1785	$(7/2,9/2)^-$	$9/2_3^-$	3.3	$p_{3/2}$	$R=4$
2127	2345	$1/2^-$	$1/2_3^-$	9.0	$p_{3/2}$	$R=2$
2220	2113	$(7/2,9/2)^-$	$7/2_4^-$	8.2	$f_{5/2}$	$R=4$
2405	2623	$(3/2,5/2)^-$	$3/2_5^-$	6.4	$f_{5/2}$	$R=4$
2429	2215	$(11/2,13/2)^-$	$11/2_3^-$	8.2	$p_{3/2}$	$R=4$
2445	2439	$(7/2,9/2)^-$	$7/2_5^-$	7.3	$p_{3/2}$	$R=4$
2636	2861	$(3/2,5/2)^-$	$5/2_6^-$	5.2	$p_{3/2}$	$R=4$

[a]Reference 5.

TABLE V. Unidentified observed positive parity states from Ref. 2 (up tp 2250 keV).

E_i	I_i^π
1327.92	$(5/2^+)$
1441.60	$(5/2)^+$
1557.87	$3/2^+$
1586.86	$1/2^+$
1635.8	$(3/2^+)$
1635.8	$(5/2^+)$
1690.70	$(5/2^+,3/2^+)$
1750.14	$(5/2)^+$
1794.6	$7/2^+$
1885.7	$(7/2,5/2^+)$
1986.30	$5/2^+$
2249.55	$3/2^+$

tage in ^{105}Ag), although the same arguments hold for mixed-j orbitals. If the Fermi surface lies below (or near) low Ω values for a particular j, high spin (aligned) and low-spin (anti-aligned) states are depressed in energy relative to the $I=j$ state. The depression of high-spin states is specifically due to the maximal effect of the Coriolis interaction. As the Fermi surface moves up to higher Ω values the effects of the Coriolis interaction diminish. The multiplet first flattens out, and then begins to exhibit odd-even staggering. To illustrate the dependence of multiplet "shapes" on the position of the Fermi surface, we have performed a series of calculations where the Fermi surface has been artificially varied from an energy well below the lowest $g_{9/2}$ orbital (the $1/2^+[440]$) to above the highest $g_{9/2}$ orbital (the $9/2^+[404]$). All other parameters were fixed at the values mentioned earlier. The resultant systematics for the $g_{9/2}$,$R=2$ multiplet is shown in Fig. 3. Figure 3(a) shows the relative energies of the five states as a function of the Fermi energy (λ), where the energy of the $9/2^+$ state has been forced to a constant value for reference. The energies of the $g_{9/2}$ Nilsson states in the basis are shown on the horizontal axis. Figure 3(b) shows the predicted shape of this $R=2$ multiplet for $\lambda=38.0$ MeV. This "arched" shape has been observed for the $h_{11/2}$,$R=2$ multiplet in the odd-neutron nucleus ^{99}Ru,[8] where the Fermi surface lies below all $h_{11/2}$ orbitals. Figure 3(c) shows the predicted shape for the opposite extreme, with $\lambda=41.5$ MeV. Here one sees that the $I=j$ and $j\pm2$ states lie at approximately the same energy, but that the $I=j\pm1$ states lie at substantially lower energies. This is the "odd-even" staggering referred to earlier. The situation expected for ^{105}Ag, where $\lambda=41.55$ MeV, is closer to the shape of Fig. 3(c). The exact extent of staggering present is very sensitive to details of the calculation, but it clearly reproduces the trends observed and shown in Fig. 2.

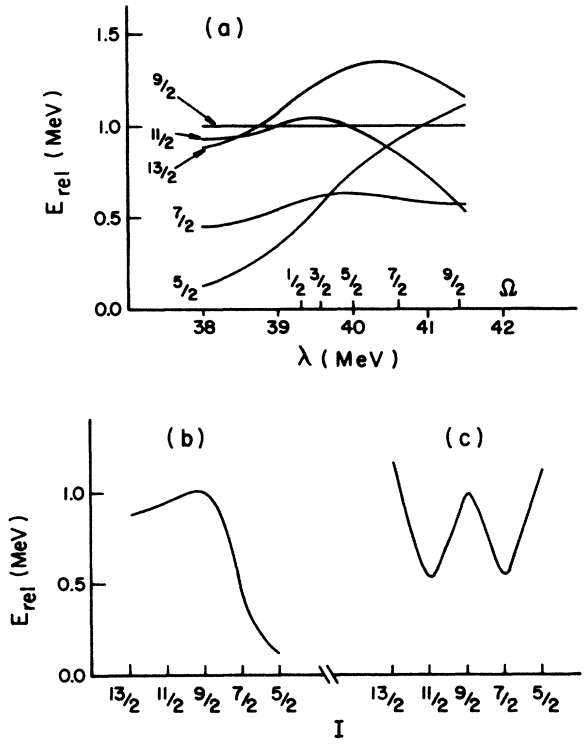

FIG. 3. Calculated systematics for the $g_{9/2}$, $R=2$ multiplet as a function of the Fermi surface λ. (a) shows relative energies of the five members as a function of λ. The energy of the $I=j$ member has been arbitrarily fixed at 1 MeV. The energies of the five Nilsson states in the basis are indicated on the horizontal axis. (b) shows the shape of the multiplet when λ is well below all the states in the basis. (c) shows the shape of the multiplet when λ is well above all the states in the basis.

V. CONCLUSIONS

A simple rotational model has been used to interpret low-lying states previously observed in ^{105}Ag with great success. A key element in the reliability of the interpretation is the ability of the model to calculate M1 transition probabilities and thus branching ratios. A new version of the popular interacting boson fermion approximation (IBFA-2),[9] in principle, has the capability to do this, but at present poorly reproduces experimental electromagnetic transition properties.[10]

The appropriateness of a rotational description of transitional nuclei such as ^{105}Ag might be questioned, since the model does not include non-rotational excitations of the core. Indeed, some of the observed states cannot be described. However, as has been mentioned earlier, the decay properties of these "non-rotational" states are very different from those of the "rotational" states, implying different wave functions. Empirically, it seems that the "degree of freedom" responsible for the "non-rotational" states does not affect the rotational degree of freedom to a great extent. The dependence on the position of the Fermi surface of the rotational systematics predicted for both yrast and non-yrast states is borne out by the experimental results. These observations argue that a rotational model will continue to be a useful tool for the understanding of transitional nuclei.

This work was supported in part by the National Science Foundation.

[1]Rakesh Popli, J.A. Grau, S.I. Popik, L.E. Samuelson, F.A. Rickey, and P.C. Simms, Phys. Rev. C **20**, 1350 (1979).
[2]S.V. Jackson, W.B. Walters, and R.A. Meyer, Phys. Rev. C **13**, 803 (1976).
[3]D. Hippe, H.-W. Shuh, B. Heits, A. Rademacher, K.-O. Zell, P.V. Brentano, J. Eberth, and E. Eube, Z. Phys. A **284**, 329 (1978).
[4]A.W.B. Kalshoven, W.H.A. Hesselink, T.J. Ketel, J. Ludziejewski, L.K. Peker, J.J. Van Ruyven, and H. Verheul, Nucl. Phys. **A315**, 334 (1979).
[5]R.M. Del Vecchio, I.C. Oelrich, and R.A. Naumann, Phys. Rev. C **12**, 845 (1975).
[6]S.G. Nilsson, K. Dan. Vidensk. Selsk. Mat.-Fys. Medd. **29**, No. 16 (1955).
[7]H.A. Smith, Jr., and F.A. Rickey, Phys. Rev. C **14**, 1946 (1976).
[8]C.S. Whisnant, R.H. Castain, F.A. Rickey, and P.C. Simms, Phys. Rev. Lett. **50**, 724 (1983).
[9]C.E. Alonso, J.M. Arias, R. Bijker, and F. Iachello, Phys. Lett. **144B**, 141 (1984).
[10]J.M. Arias, C.E. Alonso, and M. Lozano, Phys. Rev. C **33**, 1482 (1986).